Electronic Supplementary Information

Highly efficient hydrogen generation from formic acid using reduced graphene oxide-supported AuPd nanoparticle catalyst

Xinchun Yang,[a,b] Pradip Pachfule,[a] Yao Chen,[a] Nobuko Tsumori[c] and Qiang Xu*[a,b]

[a]*National Institute of Advanced Industrial Science and Technology (AIST), Ikeda, Osaka, Japan.*

E-mail: q.xu@aist.go.jp, qxuchem@hotmail.com; Fax: +81-72-751-9628; Tel: +81-72-751-9562

[b]*Graduate School of Engineering, Kobe University, Nada Ku, Kobe, Hyogo, Japan*

[c]*Toyama National College of Technology, 13, Hongo-machi, Toyama, 939-8630, Japan*

Chemicals

Natural graphite (Alfa Aesar, 325 mesh, metals basis, 99.8%), sodium nitrate ($NaNO_3$, Kishida Chemicals Co. Ltd., 99%), sulfuric acid (H_2SO_4, Kishida Chemicals Co. Ltd., 98%), potassium permanganate ($KMnO_4$, Kishida Chemicals Co. Ltd., 99.3%), hydrogen peroxide (H_2O_2, Kishida Chemicals Co. Ltd., 30%) and hydrochloric acid (HCl, Wako Pure Chemical Industries, Ltd., 35-37%) were used to prepare graphite oxide.

Potassium teterchloropalladate (K_2PdCl_4, Wako Pure Chemical Industries, Ltd., >97%), gold chloride acid ($HAuCl_4 \bullet 4H_2O$, Kishida Chemicals Co. Ltd., 99%), cobalt acetate ($Co(CH_3COO)_2 \bullet 4H_2O$, Kishida Chemicals Co. Ltd., 99%), sodium boroydride ($NaBH_4$, Sigma-Aldrich, 99%), phosphoric acid (H_3PO_4, Tokyo Chemical Industry Co. Ltd., >89%) were used to prepare the reduced graphene oxide (rGO) supported AuPd nanoparticles.

Formic acid (FA, HCOOH, Merck Millipore, 98%) and sodium formate (SF, HCOONa, Sigma-Aldrich, 99.5%) were used for hydrogen release with the catalysts.

Preparation process of $(Co_x)_EAu_yPd_{1-y}$/rGO catalysts

GO was synthesized by the modified Hummers' method[S1] and then ultrasonicated in water to form a colloidal dispersion. A mixed solution (0.06 mmol) of K_2PdCl_4 and $HAuCl_4$ with or without $Co(CH_3COO)_2$ was added into the GO dispersion (0.1 wt%, 50 mL). After adding a fresh $NaBH_4$ solution (3.7 M, 0.5 mL), the resulted mixture was stirred for 2 h. Then, the $Co_xAu_yPd_{1-y}$/rGO precipitation was separated by centrifugation. Subsequently, the precipitation was re-dispersed into 2.5 vol% H_3PO_4 (20 ml) under stirring for another 2 h. The rGO-supported AuPd nanoparticle catalyst was obtained by washing with water and centrifugation. The obtained catalyst was named as $(Co_x)_EAu_yPd_{1-y}$/rGO, where $(Co)_E$ represents the acid etching of Co, x represents the molar ratio of Co/(Au+Pd) and y is the molar ratio of Au/(Au+Pd).

Preparation process of the CO poisoned $(Co_3)_EAu_{0.6}Pd_{0.4}$/rGO catalyst

The obtained $(Co_3)_EAu_{0.6}Pd_{0.4}$/rGO catalyst was continuous stirred in a round-bottom flask (50 ml) under CO atmosphere for 1 hour. Then, the catalyst was used for the dehydrogenation of FA.

Characterization

The powder X-ray diffraction measurements were carried out using a Rigaku Ultima IV diffractometer with Cu-Kα radiation. The metal contents of the catalyst were analyzed using ICP-OES on Thermo Scientific iCAP6300. The TEM and HAADF-STEM images and EDX spectra were taken by Transmission electron microscope (TEM, TECNAI G^2 F20) with operating voltage at 200 kV equipped with energy-dispersive X-ray (EDX) detector. The N_2 adsorption/desorption isotherms were obtained at 77 K using automatic volumetric adsorption equipment (Belsorp-max). XPS spectra were recorded on a Shimadzu ESCA-3400 using an Mg Kα source. The generated gas from FA was analyzed by GC-8A (molecular sieve 5A, Ar as carrier gas) and GC-8A (Porapack N, He as carrier gas) analyzers (Shimadzu).

Catalysis activity determination

An aqueous suspension containing the as-prepared catalyst was placed in a two-neck round-bottom flask, which was placed in a water bath under ambient atmosphere. A gas burette filled with water was connected to the reaction flask to measure the volume of released gas. The reaction was started when the mixed aqueous solution of FA-SF was injected into the sealed flask to form a 4.5 mL of suspension. The molar ratio of AuPd/FA was fixed at 0.02 for all the catalytic reactions. The volume of the evolved gas was monitored by recording the displacement of water in the gas burette.

The turnover frequency (TOF) calculations

The TOF reported here is an apparent TOF value based on the number of (Au+Pd) atoms in catalyst, which is calculated from the equation as follows:

$$\boldsymbol{TOF = P_0 V / 2RTn_{AuPd}\, t}$$

where $\boldsymbol{P_0}$ is the atmospheric pressure (101325 Pa), $\boldsymbol{V}$ is the final generated volume of (H_2 + CO_2) gas, $\boldsymbol{R}$ is the universal gas constant (8.3145 m^3 Pa mol^{-1} K^{-1}), $\boldsymbol{T}$ is the room temperature (298 K), $\boldsymbol{n_{AuPd}}$ is the total molar number of (Au + Pd) atoms in catalyst and $\boldsymbol{t}$ is the completion time of the reaction in hour.

Durability test

After the catalytic reaction, the catalyst was recollected by centrifugation, washed with water and recycled for durability. In each cycle 100 % FA is decomposed, corresponding to a TON value of 50 for each cycle.

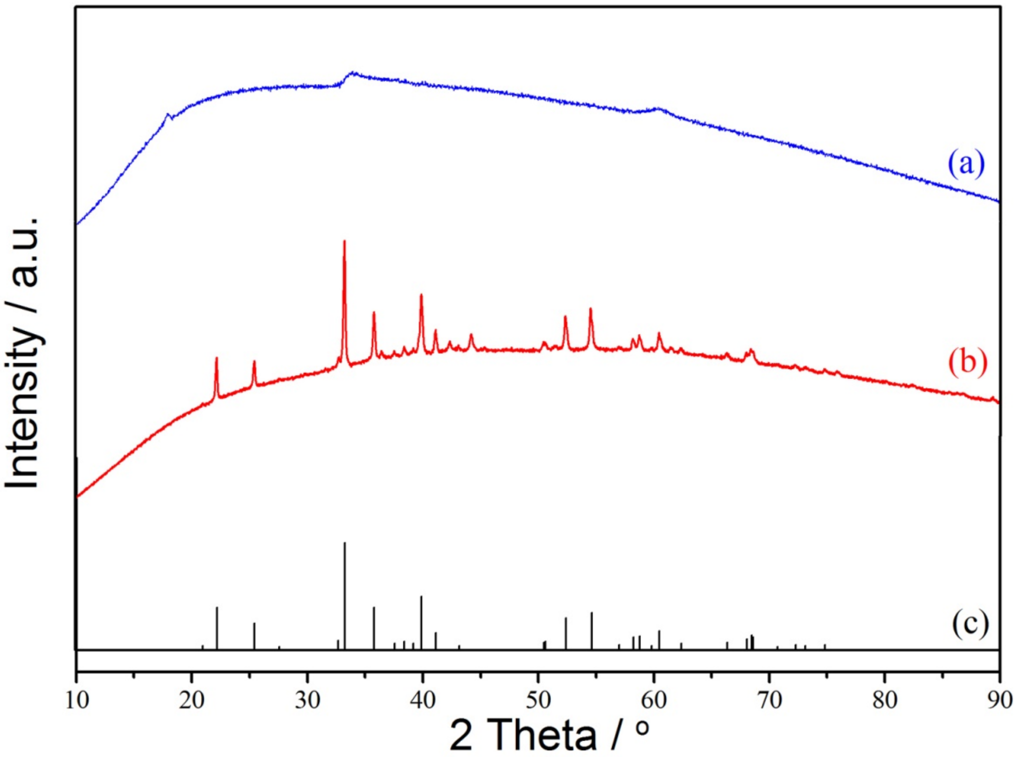

Figure S1. XRD patterns of the products from the reaction between $Co(CH_3COO)_2$ and $NaBH_4$ (a) before and (b) after annealing (823 K, 3 h, Ar), and (c) JCPDS: 25-0102 ($Co_3(BO_3)_2$).

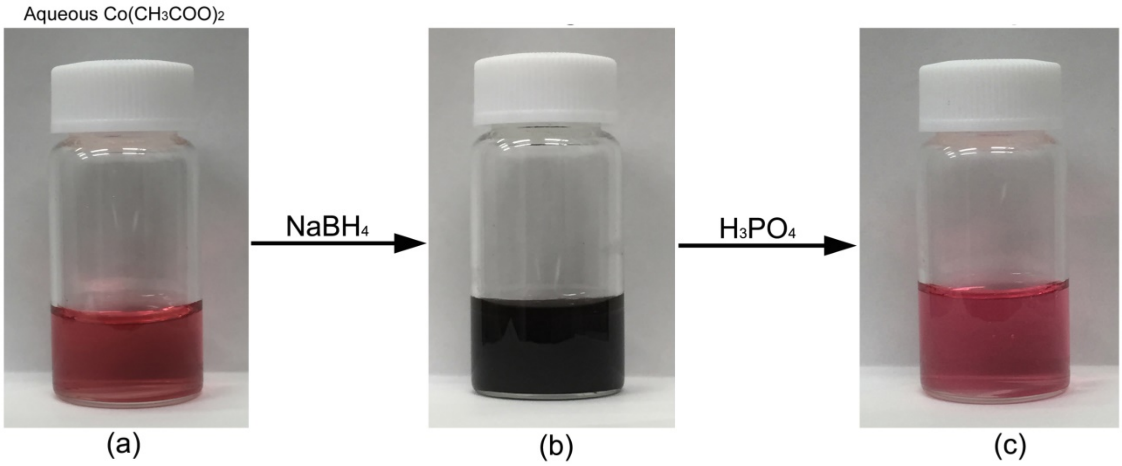

Figure S2. Photographs of (a) aqueous $Co(CH_3COO)_2$ solution and the products from the reaction between $Co(CH_3COO)_2$ and $NaBH_4$ at room temperature (b) before and (c) after etching with H_3PO_4.

The reaction between $Co(CH_3COO)_2$ and $NaBH_4$ in a molar ratio of 1:3.7 under an ambient condition for 2 h results in the formation of a black precipitation (Figure S2b), which exhibits very broad X-ray diffractions (XRD) (Figure S1a), characteristic of an amorphous phase. The sample crystallizes by annealing at 823 K for 3 h (Ar atmosphere), displaying the XRD peaks (Figure S1b) corresponding to $Co_3(BO_3)_2$ phase (JCPDS: 25-0102, Figure S1c).[S2] The precipitation $Co_3(BO_3)_2$ can be readily dissolved in H_3PO_4 (Figure S2c). Thus, in our work, the cobalt was used as the sacrificial agent for the NNMSA.

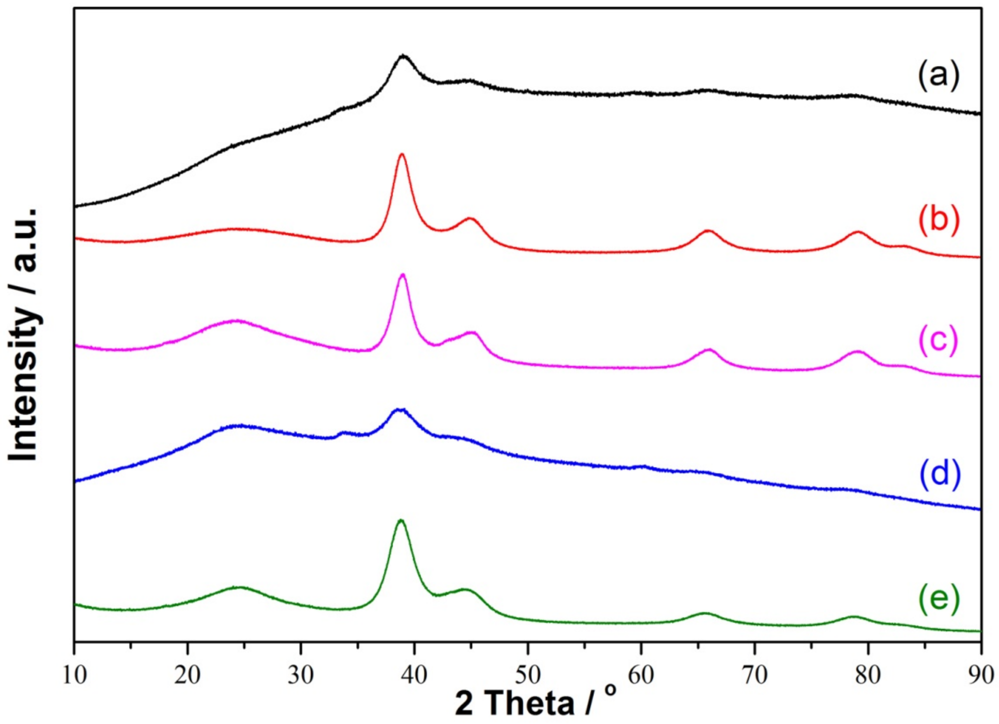

Figure S3. XRD patterns of (a) $Co_3Au_{0.6}Pd_{0.4}$, (b) $(Co_3)_EAu_{0.6}Pd_{0.4}$, (c) $Au_{0.6}Pd_{0.4}$/rGO, (d) $Co_3Au_{0.6}Pd_{0.4}$/rGO, and (e) $(Co_3)_EAu_{0.6}Pd_{0.4}$/rGO.

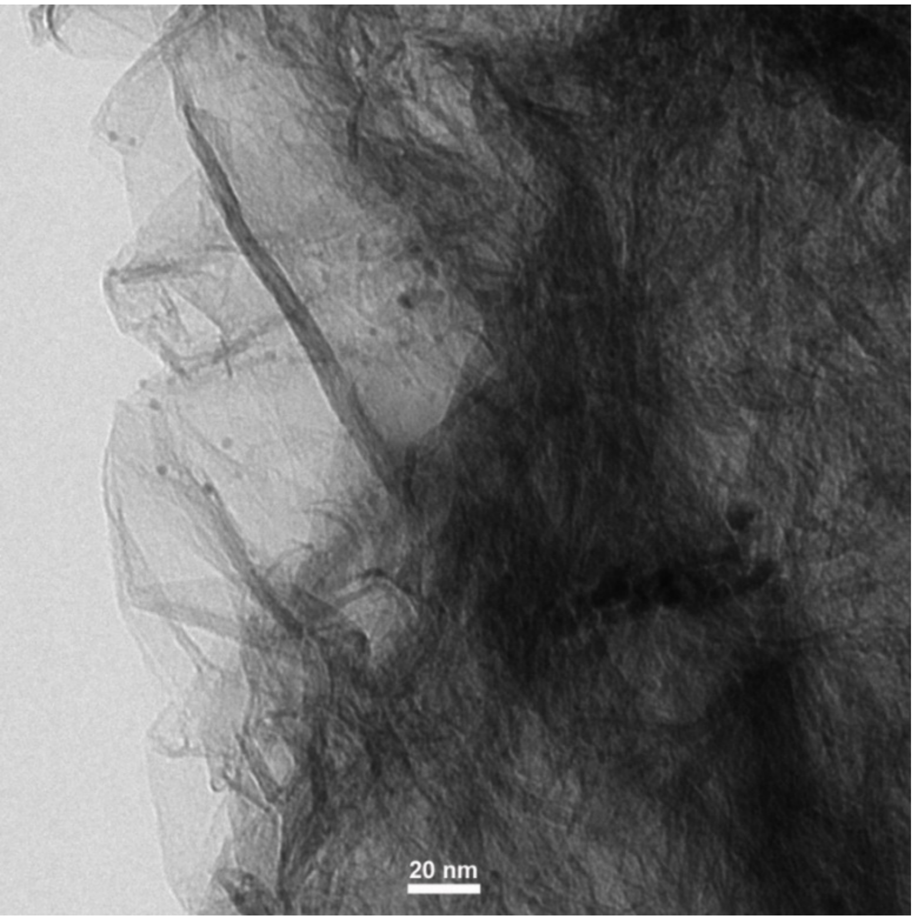

Figure S4. TEM image of $Au_{0.6}Pd_{0.4}$/rGO.

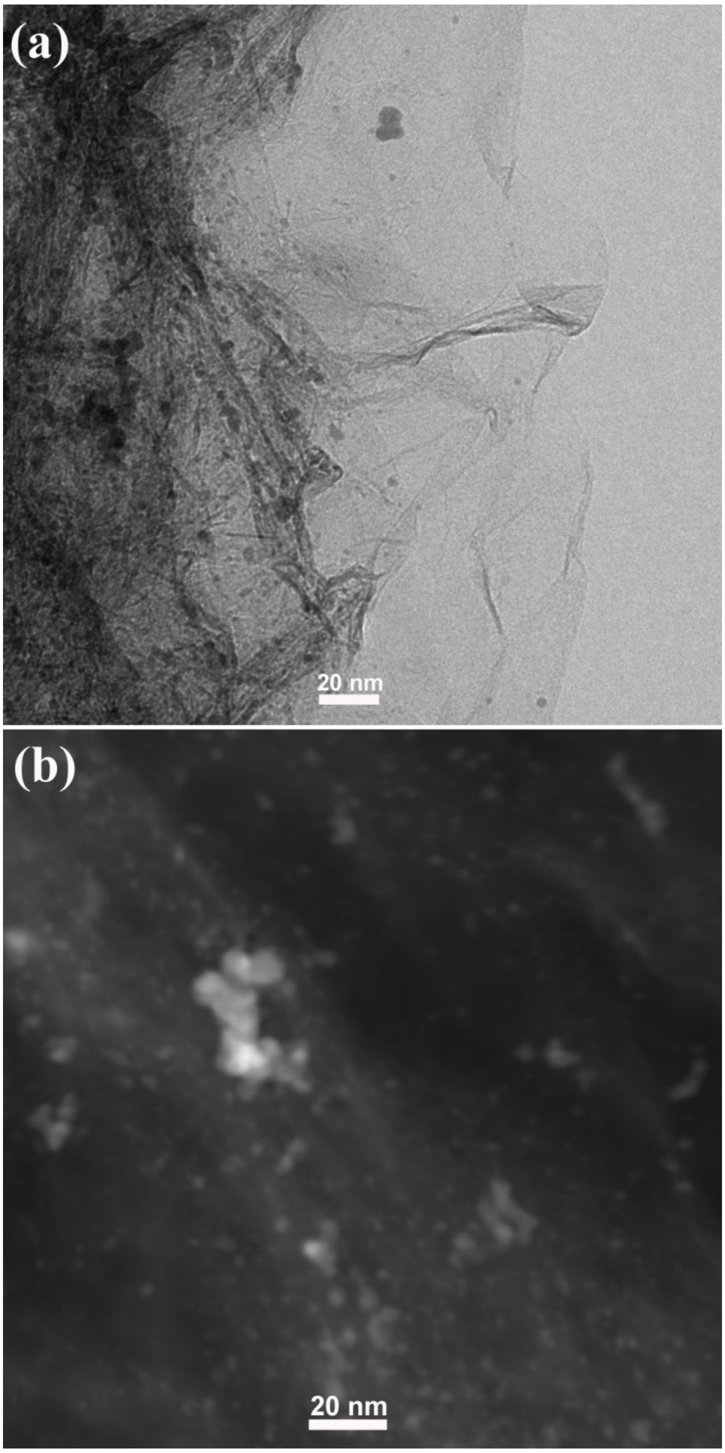

Figure S5. (a) TEM and (b) HADDF-STEM images of $Co_3Au_{0.6}Pd_{0.4}$/rGO.

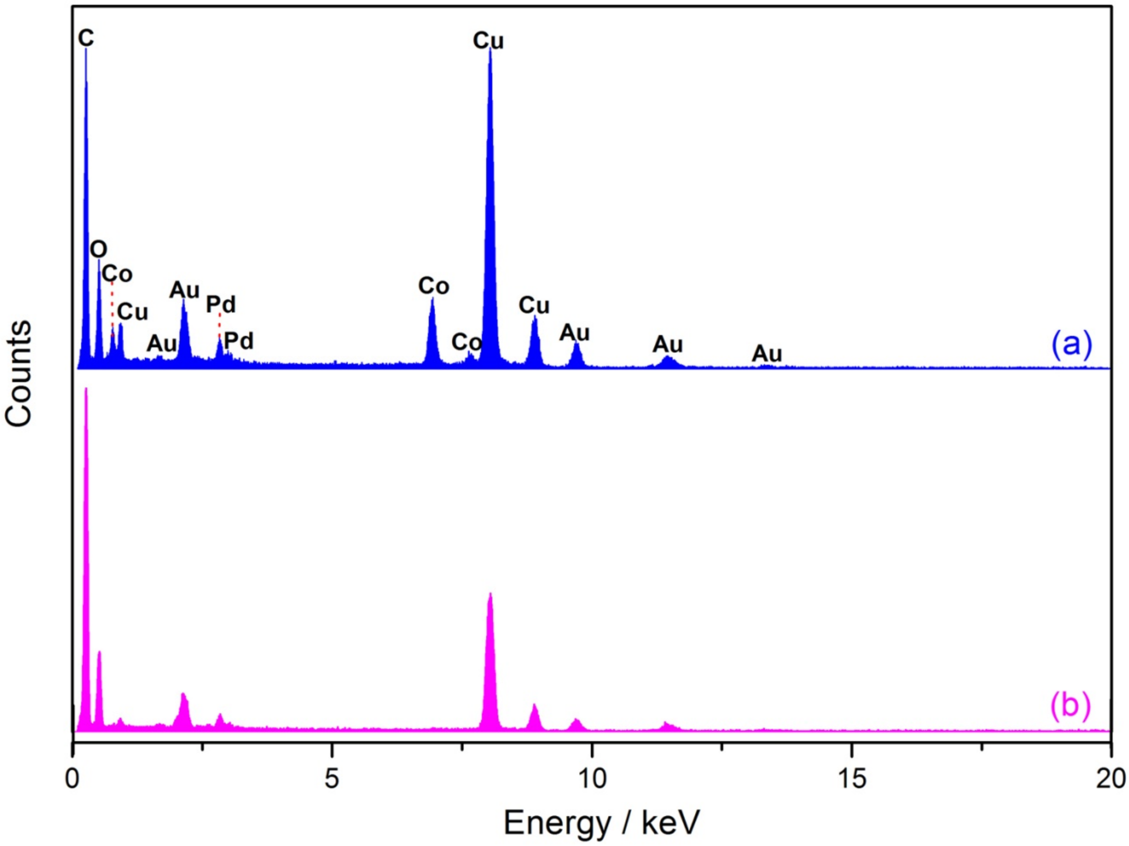

Figure S6. EDX patterns of (a) $Co_3Au_{0.6}Pd_{0.4}$/rGO and (b) $(Co_3)_EAu_{0.6}Pd_{0.4}$/rGO.

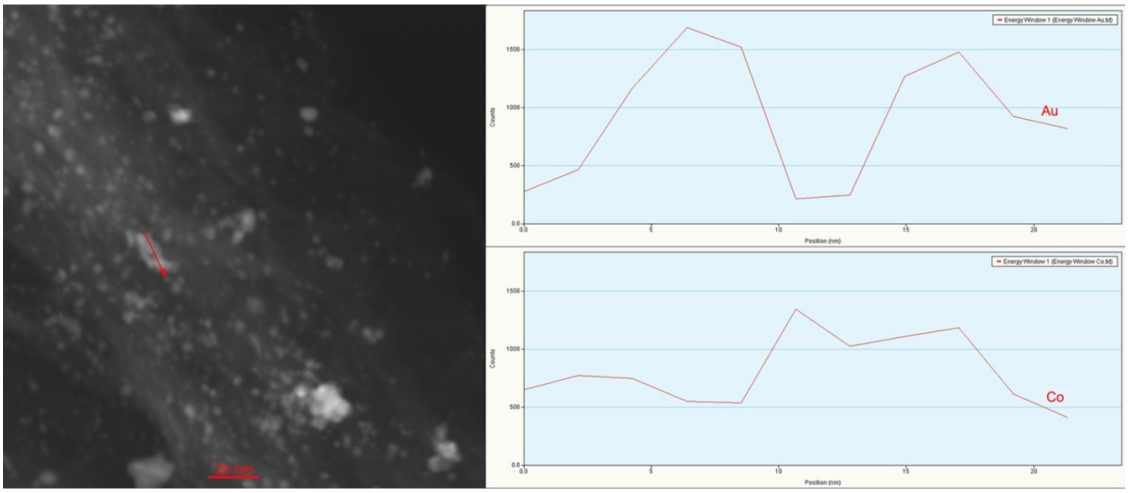

Figure S7. (a) HAADF-STEM image of $Co_3Au_{0.6}Pd_{0.4}$/rGO and (b) the corresponding EDX-line scan along the red line in (a).

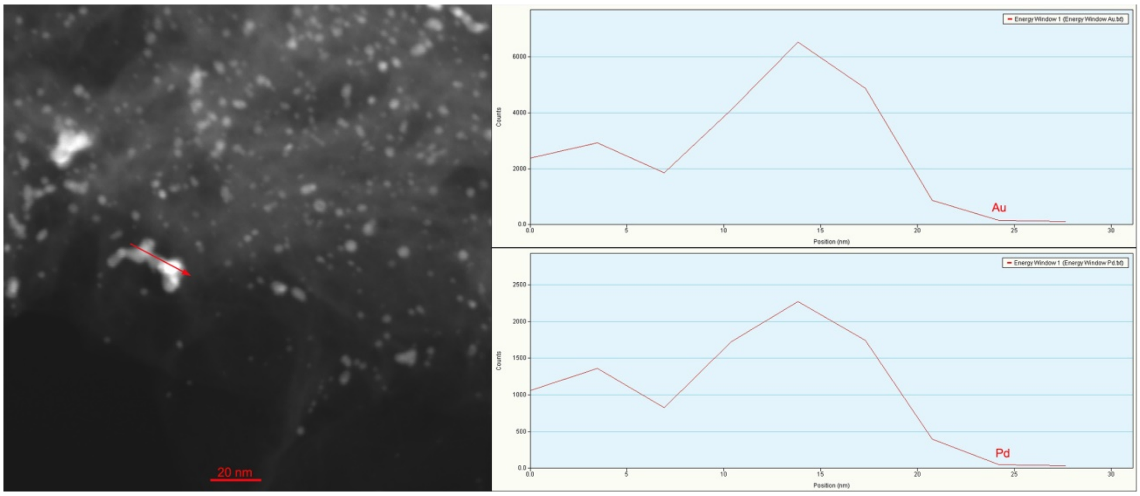

Figure S8. (a) HAADF-STEM image of $(Co_3)_E Au_{0.6} Pd_{0.4}$/rGO and (b) the corresponding EDX-line scan along the red line in (a).

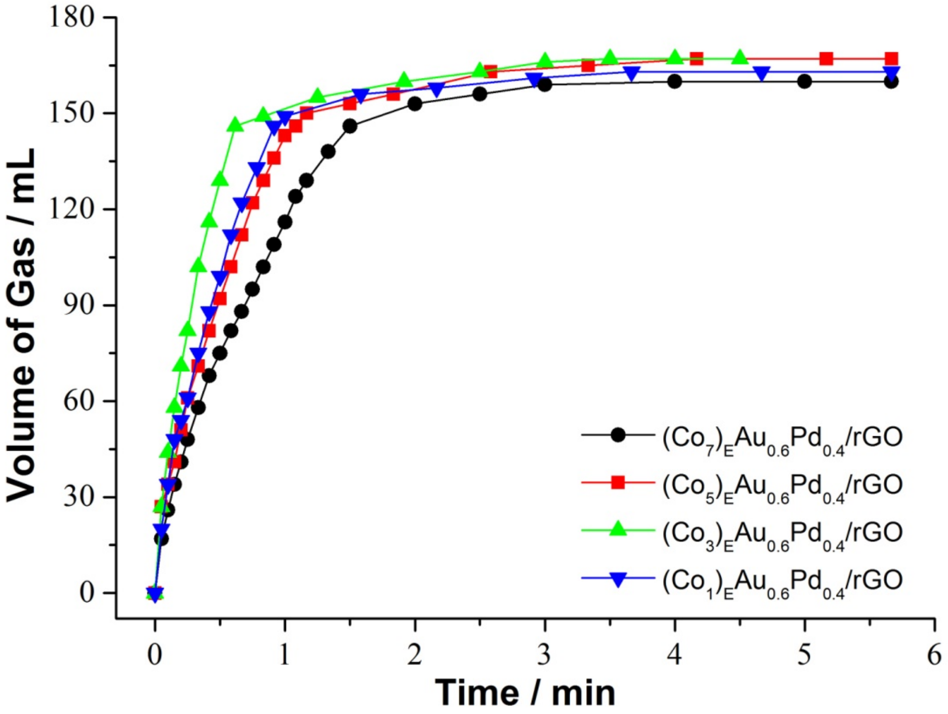

Figure S9. Volume of the generated gas (CO_2+H_2) versus time for the dehydrogenation of FA over the $(Co_x)_EAu_{0.6}Pd_{0.4}$/rGO catalyst at 323 K ($n_{AuPd}/n_{FA}=0.02$, $n_{SF}/n_{FA}=2.5$).

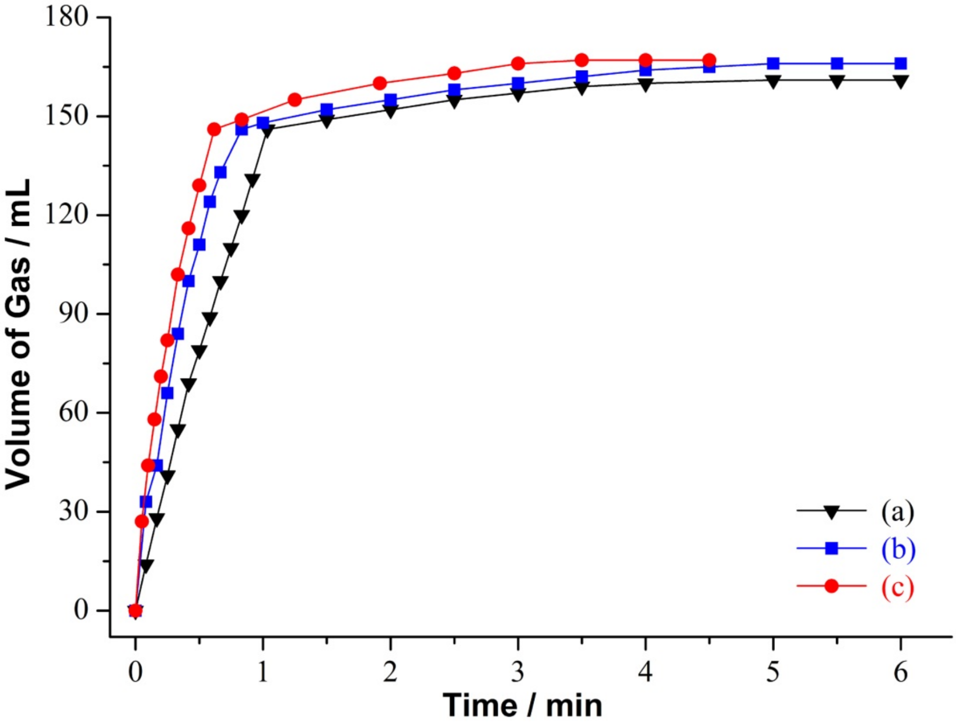

Figure 10. Volume of the generated gas (CO_2+H_2) versus time for the dehydrogenation of FA over the $(Co_3)_EAu_{0.6}Pd_{0.4}$/rGO catalyst with different loadings of metals (a) n_{AuPd} = 0.04 mmol, (b) n_{AuPd} = 0.05 mmol and (c) n_{AuPd} = 0.06 mmol and the same GO amount at 323 K (n_{SF}/n_{FA} = 2.5, FA = 3 mmol), showing TOF values of 4338, 4300, and 4840 h^{-1}, respectively.

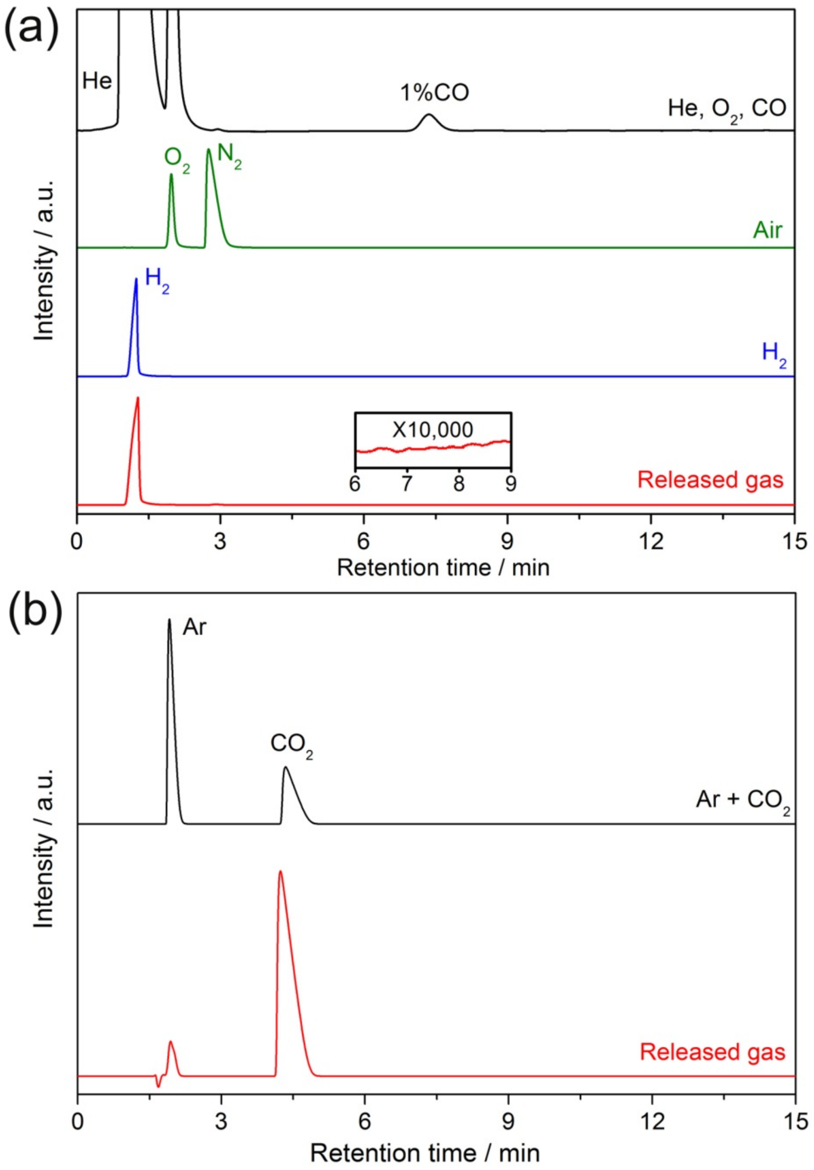

Figure S11. Gas chromatograms (GC) of the released gas (under Ar atmosphere) from the decomposition of FA in the FA/SF system ($n_{SF}/n_{FA} = 2.5$) over the $(Co_3)_EAu_{0.6}Pd_{0.4}$/rGO catalyst at 323 K with (a) CO, air and H_2 and (b) CO_2 as reference gas, indicative of the absence of CO and presence of CO_2 and H_2 in the released gas.

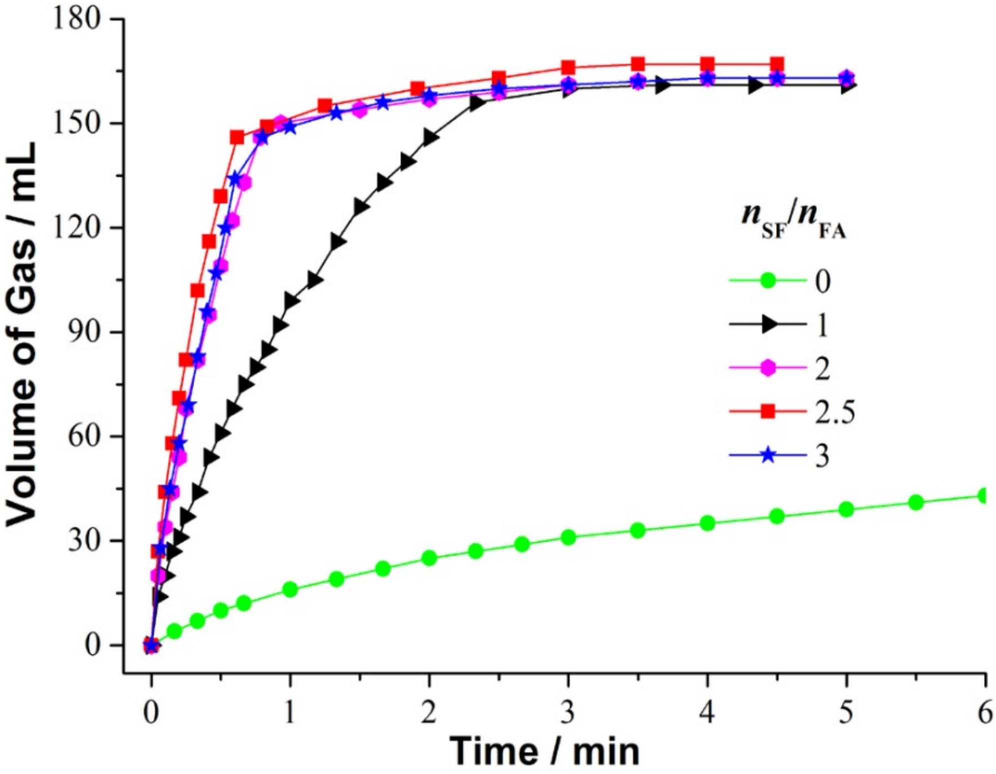

Figure S12. Volume of the generated gas (CO_2+H_2) versus time for the dehydrogenation of FA with different n_{SF}/n_{FA} molar ratios over the $(Co_3)_EAu_{0.6}Pd_{0.4}$/rGO catalyst at 323 K (n_{AuPd}/n_{FA}= 0.02).

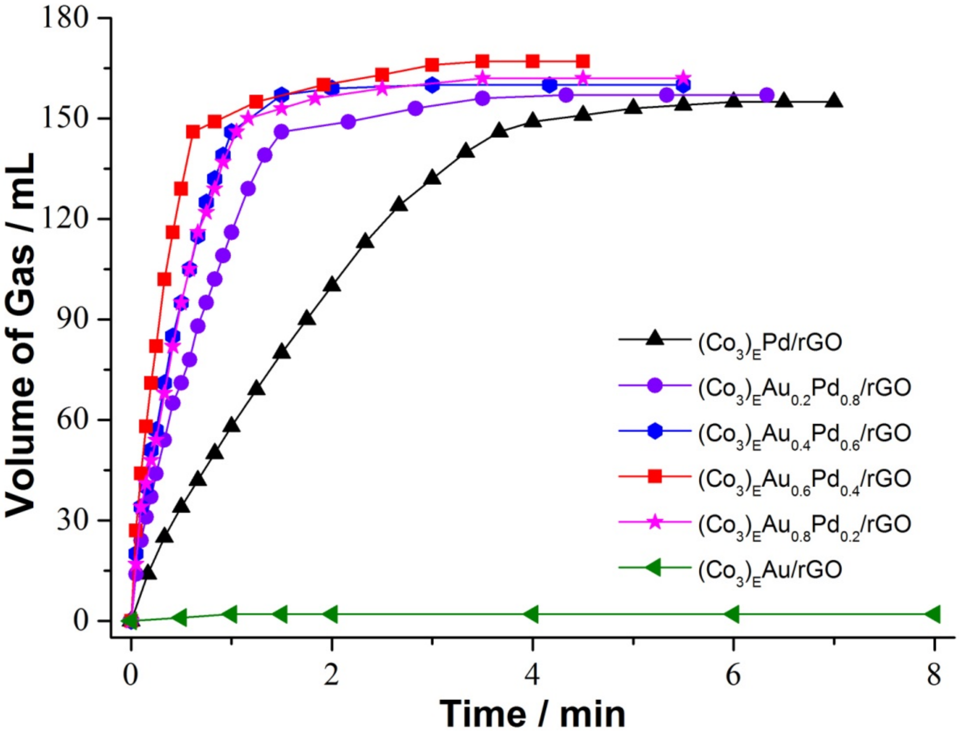

Figure S13. Volume of the generated gas (CO_2+H_2) versus time for the dehydrogenation of FA over the $(Co_3)_EAu_yPd_{1-y}/rGO$ catalysts at 323 K (n_{AuPd}/n_{FA} = 0.02, n_{SF}/n_{FA} = 2.5).

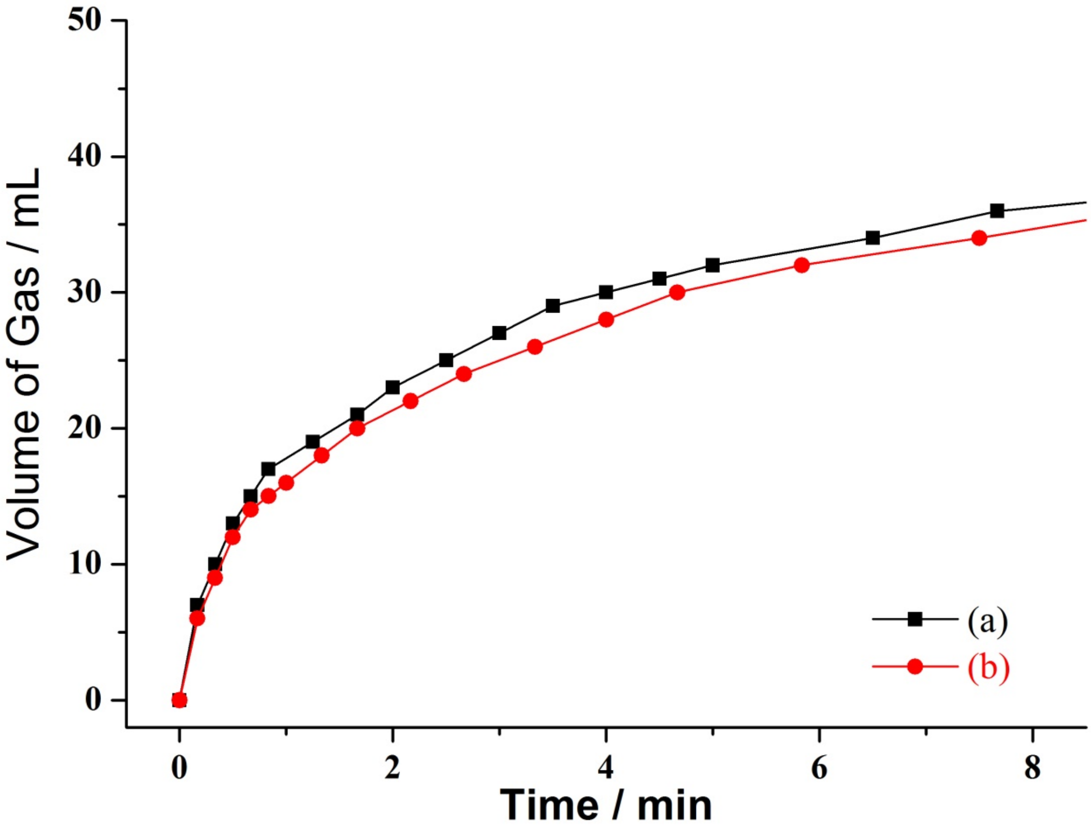

Figure S14. Volumes of the generated gas (CO_2+H_2) versus time for the dehydrogenation of FA over the support-free (a) $(Co_3)_EAu_{0.6}Pd_{0.4}$ and (b) $Au_{0.6}Pd_{0.4}$ catalysts at 323 K (n_{AuPd}/n_{FA} = 0.02, n_{SF}/n_{FA} = 2.5).

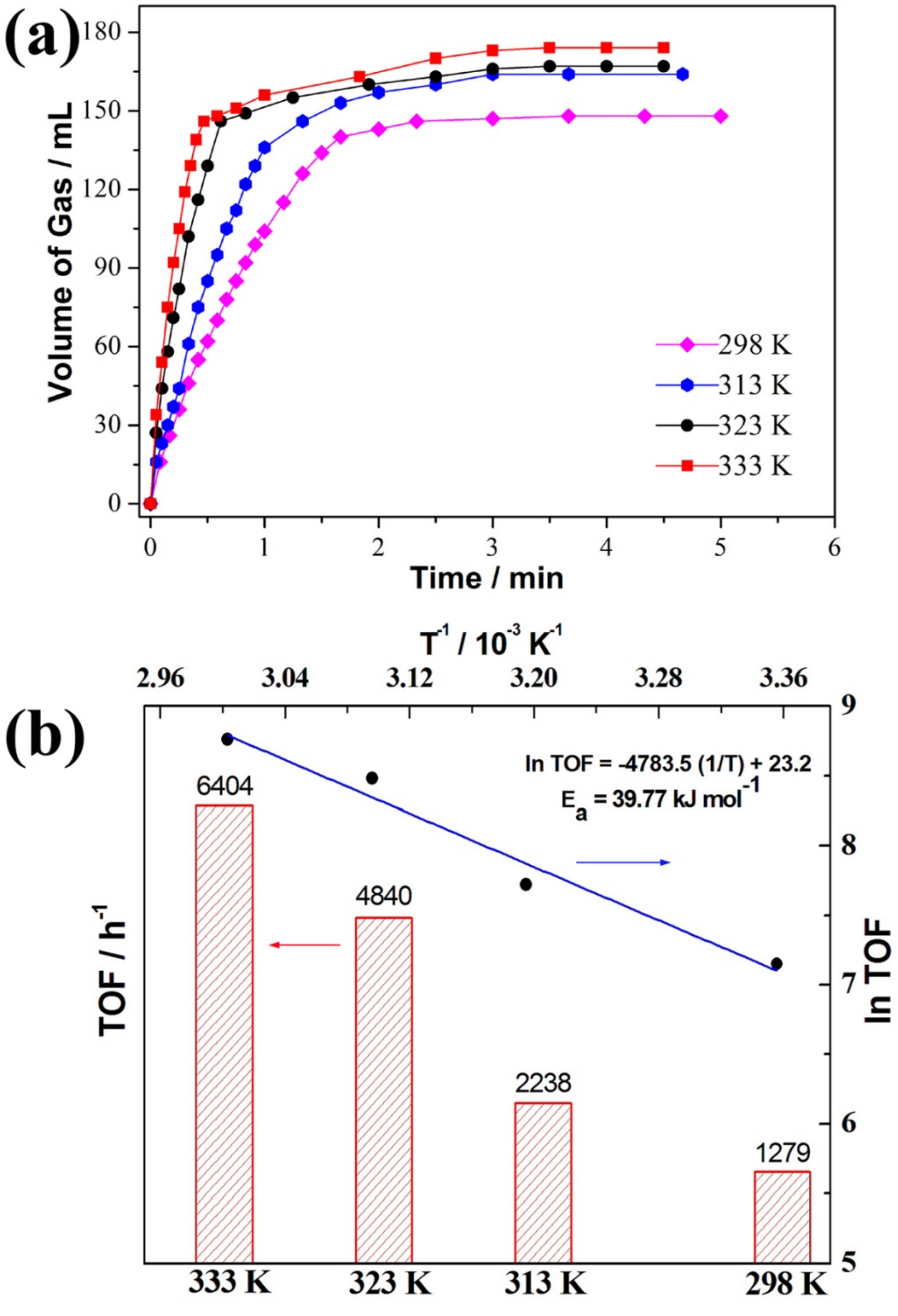

Figure S15. (a) Volume of the generated gas (CO_2 + H_2) versus time, (b) Arrhenius plot and TOF values for the dehydrogenation of FA over the $(Co_3)_EAu_{0.6}Pd_{0.4}$/rGO catalyst at different temperatures (n_{AuPd}/n_{FA} = 0.02, n_{SF}/n_{FA} = 2.5).

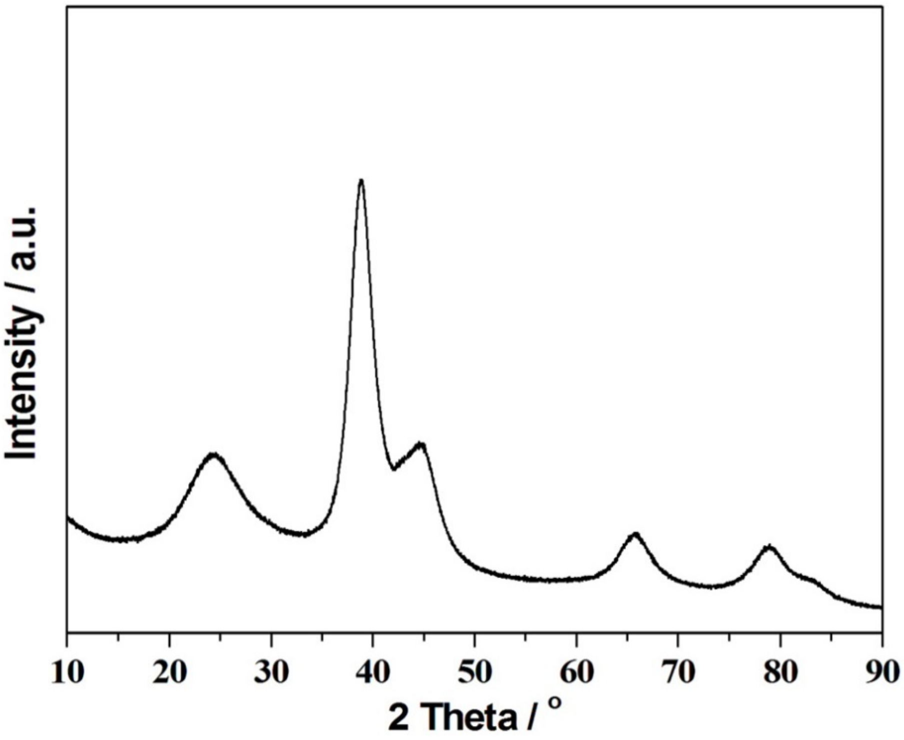

Figure S16. XRD pattern of the $(Co_3)_EAu_{0.6}Pd_{0.4}$/rGO catalyst after 5 catalytic cycles (n_{AuPd}/n_{FA} = 0.02, n_{SF}/n_{FA} = 2.5, 323 K).

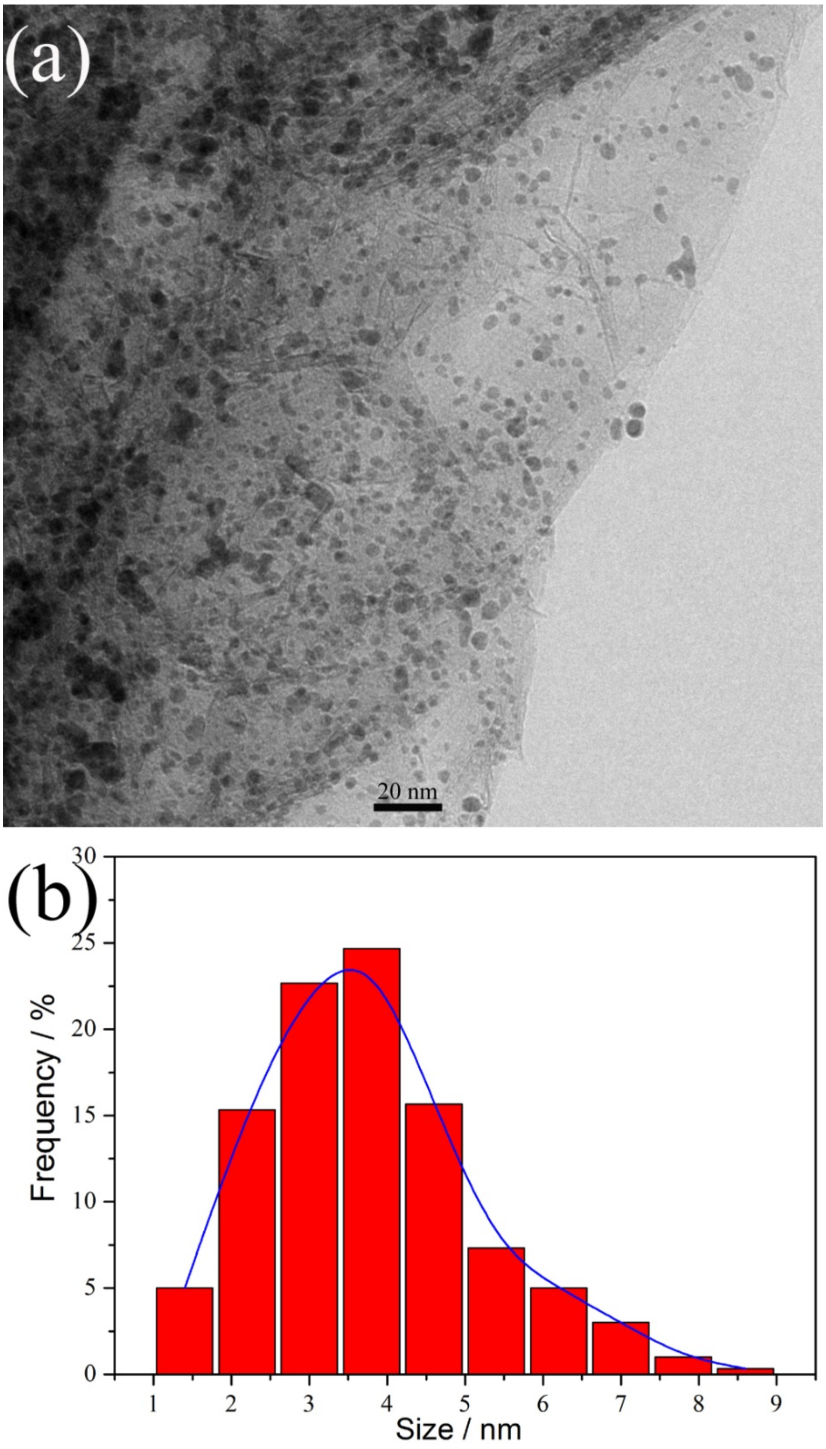

Figure S17. (a) TEM image and (b) size histogram of AuPd NPs of the $(Co_3)_EAu_{0.6}Pd_{0.4}$/rGO catalyst after 5 cycles for dehydrogenation of FA (n_{AuPd}/n_{FA} = 0.02, n_{SF}/n_{FA} = 2.5, 323 K).

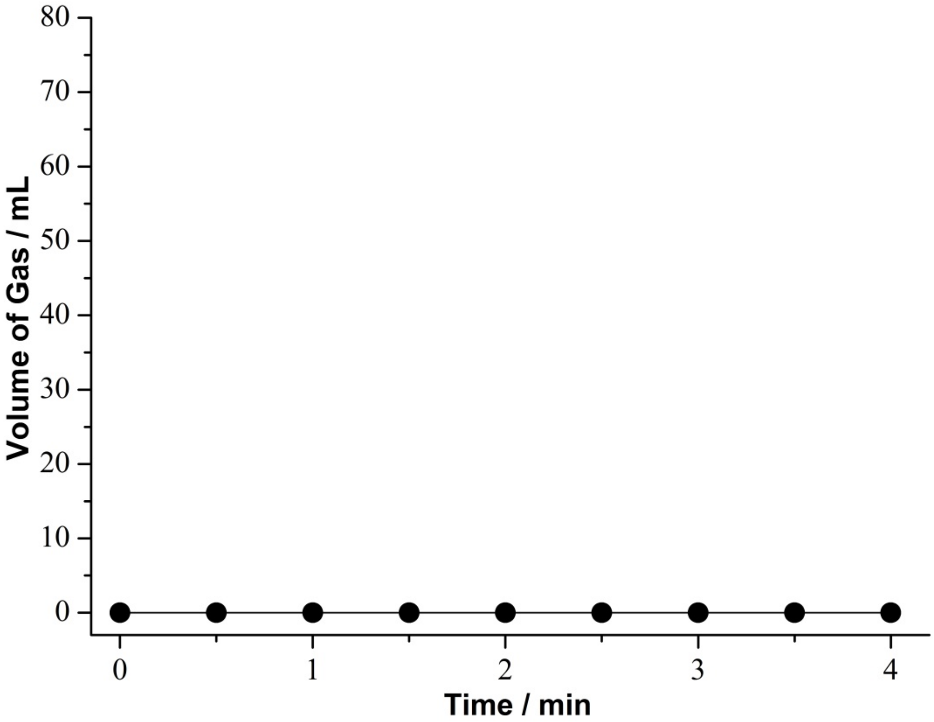

Figure S18. Volume of the generated gas (CO_2 + H_2) versus time for the dehydrogenation of FA over the CO poisoned $(Co_3)_EAu_{0.6}Pd_{0.4}$/rGO catalyst, prepared by exposing the catalyst to CO atmosphere, at 323 K (n_{AuPd}/n_{FA} = 0.02, n_{SF}/n_{FA} = 2.5).

Table S1 Catalytic activities for dehydrogenation of formic acid catalysed by related heterogeneous catalysts.

Catalyst	Solvent/medium	Temp. (K)	CO evolution	TOF (h^{-1})	Ref.
$(Co_3)_EAu_{0.6}Pd_{0.4}$/rGO	Aqueous/HCOONa	323	No	4840	This work
Pd/C_m	Aqueous/HCOONa	323	No	4452	S3
Au@ Schiff_SiO_2	Aqueous	323	No	4368	S4
Pd/PDA_rGO	Aqueous/HCOONa	323	No	3810	S5
Au@ Schiff_SiO_2	No	323	No	2882	S4
$(Co_6)Ag_{0.1}Pd_{0.4}$/rGO	Aqueous/HCOONa	323	No	2739	S6
Pd/MSC_30	Aqueous/HCOONa	323	No	2623	S7
Au/ZrO2 NCs	5HCOOH/2NEt3	323	No	1593	S8

Table S2 TOFs for the dehydrogenation of FA over $(Co_3)_EAu_{0.6}Pd_{0.4}$/rGO for the cycles of durability test (n_{AuPd}/n_{FA} = 0.02, n_{SF}/n_{FA} = 2.5, 323 K).

Cycles	TOF / h^{-1}
1st	4840
2nd	4369
3rd	4592
4th	3987
5th	4265

References

[S1] (a) W. S. Hummers and R. E. Offeman, *J. Am. Chem. Soc.*, 1958, **80**, 1339; (b) Y. Chen, X. Zhang, P. Yu and Y. Ma, *Chem. Commun.*, 2009, 4527.

[S2] G. N. Glavee, K. J. Klabunde, C. M. Sorensen and G. C. Hadjapanayis, *Langmuir*, 1992, **8**, 771.

[S3] Q. L. Zhu, N. Tsumori and Q. Xu, *J. Am. Chem. Soc.*, 2015, **137**, 11743.

[S4] Q. G. Liu, X. F. Yang, Y. Q. Huang, S. T. Xu, X. Su, X. L. Pan, J. M. Xu, A. Q. Wang, C. H. Liang, X. K. Liang, X. K. Wang and T. Zhang, *Energy Environ. Sci.*, 2015, **8**, 3207.

[S5] F. Z. Song, Q. L. Zhu, N. Tsumori and Q. Xu, *ACS catal.*, 2015, **5**, 5141.

[S6] Y. Chen, Q. L. Zhu, N. Tsumori and Q. Xu, *J. Am. Chem. Soc.*, 2015, **137**, 106.

[S7] Q. L. Zhu, N. Tsumori and Q. Xu, *Chem. Sci.*, 2014, **5**, 195.

[S8] Q. Y. Bi, X. L. Du, Y. M. Liu, Y. Cao, H. Y. He and K. N. Fan, *J. Am. Chem. Soc.*, 2012, **134**, 8926.